



A miniaturized analyzer for the catalytic determination of iodide in seawater and pharmaceutical samples

Fatima Zohra Abouhiat^{a,b}, Camelia Henríquez^b, Burkhard Horstkotte^c, Farida El Yousfi^a, Víctor Cerdà^{b,*}

^a Faculty of Sciences, Department of Chemistry, University Abdelmalek Essaadi, B.P. 2121 Mhannech II, 93002 Tétouan, Morocco

^b Department of Analytical Chemistry, University of the Balearic Islands, Carretera de Valldemossa km 7.5, 07122 Palma de Mallorca, Spain

^c Department of Analytical Chemistry, Faculty of Pharmacy, Charles University of Prague, Heyrovského 1203, 50005 Hradec Kralov, Czech Republic

ARTICLE INFO

Article history:

Received 12 December 2012

Received in revised form

22 February 2013

Accepted 28 February 2013

Available online 13 March 2013

Keywords:

Iodide

Air-bubble removal

Kinetic determination

Flow conduit

Multisyringe flow injection analysis

ABSTRACT

A monolithic flow conduit was especially designed and coupled to a multisyringe unit (MSFIA) in order to develop a kinetic analytical method. The new device, denoted CHIP, integrates different functions in a reduced size including confluent mixing, reaction coil, and thermostating, which allowed minimizing the dimensions of the entire analyzer system. The CHIP–MSFIA was satisfactorily applied to the determination of iodide using the Sandell–Kolthoff reaction. The resulting system allows fast, simple and automatic analysis in seawater samples and a pharmaceutical preparation. By the use of an additional syringe, reagent blank, sample blank, unspecific interferences, and sample analyte concentration was evaluated by simply changing the mode of operation. The instrumentation and analytical procedures were optimized in respect of sensitivity. A limit of detection of $4.7 \mu\text{g L}^{-1}$ and linear working range of $4.3\text{--}70 \mu\text{g L}^{-1}$ were achieved.

Two new modes of air bubble elimination were developed and employed in this work, leading to improved reproducibility (RSD % = 1.5%) and method robustness. The accuracy of analysis for seawater samples was evaluated by an Add–Recovery test obtaining recoveries between 97 and 106%. For the quantification of iodide in the pharmaceutical sample, standard addition calibration was required. No significant differences between the found and the certified value were found. The entire analytical procedure lasted about 150 s enabling a measuring frequency of 23 h^{−1}.

© 2013 Elsevier B.V. All rights reserved.

1. Introduction

Analytical flow techniques (FT), extensively described in distinct reviews [1–3] and monographs [4–6] are the most adequate systems for the automation of the analytical methods. Main advantages such as simplicity, efficient use of reagents and sample, and versatility, i.e. flexibility and applicability to the automation of a multitude of sample preparative procedures, detection techniques and analytes have been proven by a number of publications, which recently surpassed 20,000 [7].

One important analytical application where FT surely stands out from other approaches is kinetic determination. This is because reproducible metering and mixing of all solutions, precise timing until data readout, and shielding of the reaction mixture from outer contamination are imperative requirements, which can be perfectly fulfilled using FT. Software-configurable FT operations are possible in Sequential Injection Analysis (SIA) [8,9] or in Multisyringe Flow Injection Analysis (MSFIA) [1,10] even

allows the adaptation of the reaction conditions e.g. reaction time, sample volume, or operation scheme.

Under such strict control of the reaction's conditions, evaluation of a reaction's kinetic bears the potential of highly sensitive determination of catalyzing species. However, the most critical factor in such approaches is probably the reaction temperature, affecting (1) the reaction kinetic, (2) the viscosity of the solutions and by this the mixing conditions, (3) the gas solubility of the solutions, and (4) the refraction index of the solution, which can affect applying optical detection methods.

In this work, a monolithic flow conduit made of PMMA, following denoted CHIP was especially designed for kinetic determinations using a multisyringe pumping unit for solution handling leading to a robust and simple MSFI-Analyzer. Monolithic flow conduits have been former reported as the possibility to integrate different functions in one single and purpose-made flow devices [11–14] which finally has led to the multi-purpose monolithic conduit known as Lab-on-Valve (LOV) [3,15].

The objective of the presented work was the development of a miniaturized analyzer system by reducing manifold dimensions, improvement the robustness of the manifold configuration and the mixing efficiency of the implied reagents, and, in particular, by strict temperature control of the integrated reaction coil.

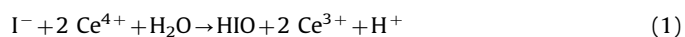
* Corresponding author.

E-mail address: victor.cerda@uib.es (V. Cerdà).

MSFIA can be considered as an ideal choice for the solution propelling in kinetic measurements since it offers the possibility of simultaneous propulsion of up to four different solutions, e.g. sample and reagents, in a smooth, homogeneous, and pulse-less flow mixed in constant ratio. Further characteristics is the individual activation or de-activation of each pumping channel (multi-commutation) and operation over a wide, computer-controlled and reliable flow rate range without affected by neither flow resistance nor sample viscosity. This allows homogeneous and highly reproducible mixing of the implied solutions, an imperative requirement for kinetic determinations. Multi-commutation is of special interest for improving the methods of performance. It allows flow stop operations and minimizes the reagent consumption by zone-merging of sample and reagent instead of continuous confluence of the reagent to the carrier flow.

In addition to the CHIP design, we propose two simple approaches for partial reagent and carrier degassing, air bubble removal and decreased air bubble stacking which improved greatly the robustness of the analyzer operation.

To prove the usefulness of the combination of MSFIA with the designed CHIP, the system was applied to the kinetic determination of iodide using the Sandell–Kolthoff reaction [16] with the Ce(IV) reduction followed by spectrophotometric detection. In 1934, Sandell and Kolthoff described the catalytic effect of iodide on the Redox-reaction between Ce(IV) and As(III). Later, Stanley and Thomas [17] proposed a complex reaction mechanism indicating that only iodide itself but not iodine catalyses the oxidation of As(III) to As(V) and that acidity of the reaction mixture would increase. Although the mechanism of the reaction seems to be not well established yet, it is an accepted standard reaction for the determination of iodide and has been widely applied to different samples due to its high sensibility and selectivity [18,19].



Iodine is an essential element for the human health as is a part of the thyroid hormones participating in the regulation process of the cell metabolism. It shows similar importance for numerous biological systems [20–22]. As nutrient additive, it is gained especially from macro-algae. Iodine is present in low concentrations in soils and is also found in seawater in concentration in order of 50 ppb in the mixed ocean surface layer, expressed as total iodine, i.e. iodide and iodate.[19,23]. Monitoring of iodide concentration in different kinds of samples including pharmaceutical preparations and dietetic complements [24,25], biological fluids [22,26,27], seawater [20,28], drinking water [29] has an increasing attention.

A variety of analytical methodologies have been proposed for iodide determination, including manual [24,30], automated [15,19,23,25,26] and chromatographic methods [19,27]. Used detection techniques included voltamperometry [27], potentiometry with ion-selective electrodes [31], thermometry [26], ICP-MS [18], chemiluminescence [22], ion chromatography [32,33] capillary electrophoresis [34], and most widely used, spectrophotometry [16,18,19,22,26,28,29]; based on the Sandell–Kolthoff reaction to a significant percentage. For more details, the reader is referred to an IUPAC report [19] and an extensive review article on this topic [18]. However, none of these studies have resulted in a portable system able to perform on-board iodide measurement. In this sense, the proposed analyzer offers the potential of in field application of iodide monitoring. Considering the toxicity of the required reagents for the Sandell–Kolthoff reaction but the common use as reference of this method, it is obvious that miniaturization of the manual method with the aim of a simpler, less expensive, and minimal consumption of the reagents is

appealing. Further requirements such as accurateness, rapidness, and automation are evident.

2. Materials and methods

2.1. Reagents and standards

Purified milliQ water was used throughout for preparation of all the solutions. For the preparation of analytical standards, 0.131 g of potassium iodide, previously dried at 110 °C, were precisely weighed and dissolved in 100 mL of milliQ water obtaining a 1.001 g L⁻¹ iodide stock solution. Working standards were prepared by successive dilutions of the stock solution.

Stock solutions of 5 mol L⁻¹ sulfuric acid and 5 mol L⁻¹ nitric acid were prepared by appropriate dilution of commercial concentrated acids of analytical reagent grade purity. Acidic reagent solutions of Ce(IV) and As(III) were prepared daily by appropriate weighing of (NH₄)₄Ce(SO₄)₄ · 2 H₂O and NaAsO₂ in diluted sulfuric or nitric acids and kept in dark until used. Optimized composition of the reagents were 3.5 mmol L⁻¹ of Ce(IV) and 10 mmol L⁻¹ of As(III) in each 0.27 mol L⁻¹ sulfuric acid.

Synthetic seawater (SSW) was prepared according to the recommendations given elsewhere [30] by dissolving the following components in milliQ water with given final concentrations: 3.0 mg L⁻¹ NaF, 20 mg L⁻¹ SrCl₂ · 6H₂O, 30 mg L⁻¹ H₃BO₃, 100 mg L⁻¹ KBr, 700 mg L⁻¹ KCl, 1470 mg L⁻¹ CaCl₂ · 2H₂O, 4000 mg L⁻¹ Na₂SO₄, 10.8 mg L⁻¹ MgCl₂ · 6 H₂O, 23.5 mg L⁻¹ NaCl, 20.0 mg L⁻¹ Na₂SiO₃ · 9H₂O, and 200 mg L⁻¹ NaHCO₃. All given reagents were purchased from Scharlau SA (Barcelona, Spain).

A 5 wt % solution of Nafion perfluorinated ion exchange resin in lower aliphatic alcohols was purchased from Sigma Aldrich (CITY, Germany) and used for PTFE coating as described in Section 3.2.

A solution of 0.5 mg L⁻¹ indigo carmine Panreac SA, (Barcelona, Spain) was used as visualization aid to adjust the operational volumes and to observe the flow pattern in the CHIP.

2.2. Flow conduit chip

The CHIP, shown schematically in Fig. 1, was especially made of three PMMA pieces of 85 × 44 × 10 mm. Throat holes for UNF ¼" 28 fittings were made in the upper part to connect the supply tubes for reagents and sample/carrier as well for the outflow to the detection flow cell. On its opposite (bottom) side, a confluence and a serpentine reaction coil of 0.8 × 0.8 mm were made using a 3-axis CNC controlled milling machine. The middle piece was then glued to cover the flow circuit applying a thin film of acrylic acid prior to tight fixation and a curing time of 1 h. In order to obtain a cavity below the flow circuit for the circulation of thermostat water, in the bottom piece as well as in the already glued assembly, two rectangular deepenings of 50 × 30 × 8 mm were milled prior to gluing both together. After curing, two flow connectors were attached to allow continuous flushing of the cavity with water provided by a peltier heating bath (PT31, Krüss Optronic, Hamburg, Germany, type PT-31) via silicon tubes (ca. 20 cm, 1 cm id). By this, the cavity served as a heating source to accelerate the reaction in the flow circuit. The temperature of the PT31 was set to its maximum of 40.0 °C.

2.3. Flow analyzer

The implemented MSFIA system for the determination of iodide is shown in Fig. 1. All liquid contacted parts were chemical resistant polymers, namely, ETFE, PMMA, and PTFE. PTFE tubing of 0.8 mm id was used for the flow lines of the manifold.

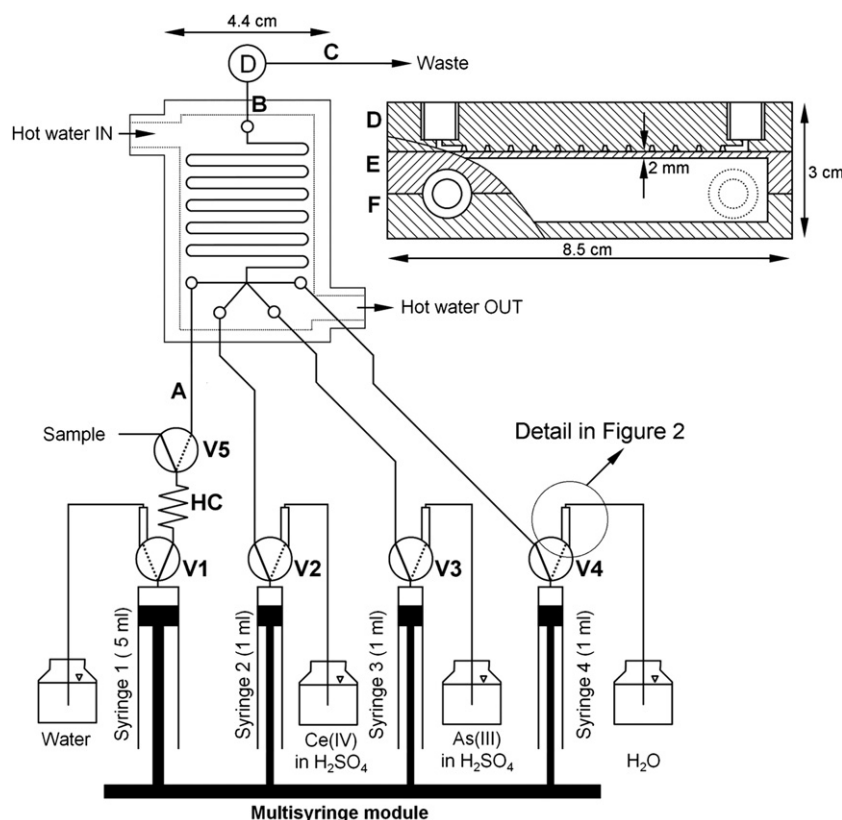


Fig. 1. Scheme of the analytical system used for the kinetic determination of iodide with detailed technical drawing of the used monolithic flow conduit (side-view). Air bubble traps are given as rectangles on the solenoid head valve. HC: 1 m holding coil of 130 cm and 0.8 mm id, V: solenoid valve, tubing lengths (id 0.8 mm) A: 8 cm, B: 12 cm, C: 60 cm, D–F: top, middle, and bottom parts of the CHIP made of PMMA and glued together with UV cured methacrylic acid.

A multisyringe piston pump module (model Bu 4S) was purchased from Crison Instruments S.A. (Allela, Barcelona, Spain). The module was equipped with three glass syringes of 1 mL (S2, S3, and S4) and one glass syringe of 5 mL (S1), all of TLL SYR series from Hamilton Bunaduz AG (Bunaduz, Switzerland).

Solenoid head valves (V1, V2, V3, and V4) allowed the connection of each syringe either with the CHIP replacing the normal tubing manifold (position ON, activated) or with the respective solution reservoir (position OFF, deactivated) for refilling. Used solutions in the syringes were Milli-Q water in S1 and S4, As(III) reagent in S3, and Ce(IV) reagent in S2. A further external three-way solenoid valve (V5) from Takasago (Nagoya, Japan, type: STV-3-1/4UKG) was powered and controlled via an auxiliary supply port of the multisyringe module. It was used for the aspiration of sample and was connected in common position via a holding coil of 1.3 mm, 0.8 mm id to position ON of V1, and in position OFF to the flow conduit via PTFE tubing of 8 cm, 0.8 mm id.

For real sample analysis, a 45 position rotary autosampler for 10 mL sample vials from Crison Instruments S.A. was placed at the sample provision tube. The multisyringe module and the autosampler were connected in series via a RS232C serial interface to a PC for remote software control (see Section 2.4).

An USB-2000 miniature CCD spectrophotometer from Ocean Optics Inc. (Dunedin, FL, USA) was used as a detector. It was directly coupled to a PMMA cell support (Sciware Systems SL, Palma de Mallorca, Spain) holding a 10 mm path-length flow cell from Starna (type 75.1 SOG, Essex, UK). Measurement parameters were 60 ms integration time and averaging three measurements with a measuring frequency of 8 Hz. A wavelength smoothing over 9 array pixels corresponding to a slight width of about 12 nm was done. A quartz glass optical fiber of 400 μ m core diameter

from Ocean Optics Inc. was used to connect the cell support to a DH-2000 Deuterium light source from TOP Sensor Systems (Eerbeek, Netherlands).

An analytical wavelength of 380 nm was used. A signal correction of unspecific effects such as fluctuations of the light source intensity or alteration of the solution refraction index was done by subtraction of the absorbance measured at a reference wavelength of 470 nm where the Ce(IV) ion does not show any significant absorbance.

2.4. Software

The software package AutoAnalysis 5.0 (Sciware Systems SL) was used for instrumental control as well as for data acquisition and treatment. The basic software protocol is adaptable to the individual instrumental assembly by incorporation of dynamic link libraries, which are amenable to communicate with the individually assembled instruments. User-friendly software tools for method development and automated optimization experiments such as loops, procedures, variables, user inquiries, waiting steps, and definition of conditional inquiries are available.

2.5. Analytical protocol

The analytical protocol of the MSFIA system is shown in Table 1. A volume of 190 μ L sample was aspirated from V5 (step 2). Then, this volume was pushed toward the CHIP (step 4) and then pushed into the reaction coil inside the CHIP after the confluent mixing with the reagents (step 5). After refilling the syringes (step 6) and incubation for 120 s at 40 $^{\circ}$ C (step 7), the reaction mixture was pushed through the detection flow cell for spectrophotometric quantification of the remaining Ce(IV)

concentration in the reaction mixture (steps 9–11). Additional steps were required to overcome the syringe pump backlash (steps 1, 3, and 8) performing a small flow operation in head valve position OFF in the same direction (dispense or pickup) as in the subsequent step.

2.6. Data evaluation

Since the proposed method is based on the reduction of Ce(IV) (chosen wavelength of 380 nm) to Ce(III) by As(III) catalyzed by iodide, the analytical signal results from the discoloration of the solution due to the given reaction schemes (1) and (2). All other ions participating or resulting from the reaction, i.e. being Ce(III), iodide, As(III) and As(V), do not absorb at the analytical wavelength.

The calibration curve had a negative slope with the blank solution giving the highest signal due to the lack of catalyst for the reduction of Ce(IV), i.e. the decrease of the chromophore. As a result, the ratio between blank signal and standard or sample signal was used for quantification.

To allow an accurate quantification, step 5, which corresponds to the mixing of the sample with the reagents, was performed in three different modes (step 5A, B, or C). Fig. 2 displays a diagram of the mathematical construction for calibration, sample

measurement, and standard addition, resulted from the application of these three modes. In mode A, the blank of reagent, i.e. the obtained signal in absence of the sample matrix, was measured. For this, a mixture of As(III), Ce(IV) and water (carrier in S1) instead of sample were used. The signal obtained with this mode was called $Abs_{(W+As+Ce)}$ corresponding to the maximal obtainable signal from Ce(IV).

In mode B, the sample, the Ce(IV) reagent, and water from S4, instead of As(III) from S3, were mixed inside the CHIP. This mode allowed the estimation of analyte-unspecific reduction of Ce(IV), while the Sandell-Kolthoff reaction cannot take place due to the absence of As(III). Unspecific reduction can be caused by the presence of reducing compounds in the sample. The obtained signal was denoted as sample blank or $Abs_{(S+W+Ce)}$. This mode also takes into account any increase of the absorbance originated from turbidity or sample hue. Thus, the signal difference between mode A and B allows the calculation of the sample contribution due to matrix absorbance or unspecific reactions $[Abs_{(W+As+Ce)} - Abs_{(S+W+Ce)}]$.

In mode C, both reagents, As(III) and Ce(IV), were mixed with the sample and measured under the same conditions as commented above. Consequently, the reaction between As(III) and Ce(IV), catalyzed by the iodide present in the sample, takes place and leads to a signal denoted as $Abs_{(S+As+Ce)}$. In addition, also unspecific

Table 1
Measurement procedure for the determination of iodide.

Steps	Device*	Operation**	Comments
1	MS	Pickup 0.150 ml at 3.750 mL/min [1-Off 2-Off 3-Off 4-Off 5-Off]	Refilling of syringes
2	MS	Pickup 0.190 ml at 3.750 mL/min [1-Off 2-On 3-Off 4-Off 5-On]	Aspiration of sample
3	MS	Dispense 0.050 ml at 3.750 mL/min [1-Off 2-Off 3-Off 4-Off 5-Off]	Overcoming of syringe pump backlash
4	MS	Dispense 0.050 ml at 3.750 mL/min [1-Off 2-On 3-Off 4-Off 5-Off]	Dispense sample to chip
5A	MS	Dispense 0.190 ml at 2.500 mL/min [1-On 2-On 3-On 4-Off 5-Off]	Mixing of sample with both reagents (S2 and S3 dispensing toward chip)
5B	MS	Dispense 0.190 ml at 2.500 mL/min [1-On 2-On 3-Off 4-On 5-Off]	Mixing of sample with Cerium alone (using water from S4 instead of S3)
5C	MS	Dispense 0.190 ml at 2.500 mL/min [1-On 2-Off 3-On 4-On 5-Off]	Mixing of sample with Arsenic alone (using water from S4 instead of S2)
6	MS	Pickup 0.900 ml at 10 mL/min [1-Off 2-Off 3-Off 4-Off 5-Off]	Refilling of syringes
7	Wait	Wait 120 s***	Reaction time
8	MS	Dispense 0.050 ml at 3.750 mL/min [1-Off 2-Off 3-Off 4-Off 5-Off]	Overcoming of syringe pump backlash
9	D	Start measure with 3.3 Hz: absorbance difference: 380–470 nm	
10	MS	Dispense 0.900 ml at 3.750 mL/min [1-Off 2-On 3-Off 4-Off 5-Off]	Measure absorbance during expulsion of reaction mixture to waste
11	D	Stop measure	

* D= Spectrophotometer USB 2000, MS= Multisyringe pump

** All volumes and flow rates refer to the size of syringe 1 (sample, 5 mL). For syringe 2, 3, and 4, used for reagents and water, volumes and flow rates are fivefold lower.

*** The reaction time is easily changeable following the requirement of analysis, in order to increase the sensitivity but to the cost of sample throughput.

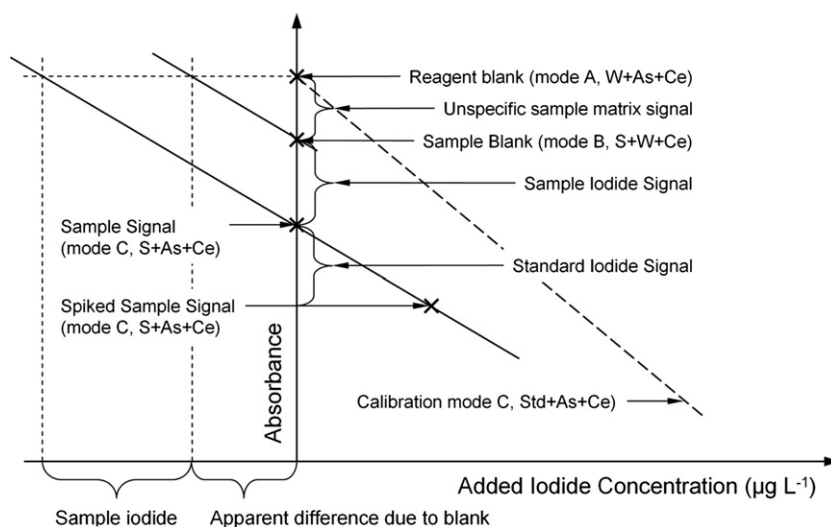


Fig. 2. Mathematical construction of calibration, sample measurement, and standard addition for quantification of iodide. All curves have negative slope due to the catalytic effect of iodide on Ce(IV) reduction.

reactions caused from the sample matrix occur. In this way, the absorbance resulted from the presence of Abs iodide (Abs_{iodide}) and its concentration in the sample can be calculated using Eqs. (3) and (4). Mode C was applied for the measurement of the original and the spiked samples, as well as the standards of the calibration curve.

$$Abs_{\text{iodide}} = Abs_{(W+As+Ce)} - [Abs_{(S+As+Ce)} + (Abs_{(W+As+Ce)} - Abs_{(S+W+Ce)})] \quad (3)$$

$$[I^-] = -Abs_{\text{iodide}} / \text{Slope} \quad (4)$$

Following these equations, three cases are possible according to the characteristics of the sample matrix. In the first and the most simple case, there is no matrix effect and no unspecific reduction of Ce(VI). Then, the signal obtained in mode A and mode B will not be significantly different, i.e., $Abs_{(W+As+Ce)} = Abs_{(S+W+Ce)}$; and the Abs_{iodide} will be the difference between the signal obtained with mode A and mode C, Eq. (5). In this case, the interpolation in a calibration curve can be used to quantify the iodide concentration as it is shown in Eq. (4).

$$Abs_{\text{iodide}} = Abs_{(W+As+Ce)} - Abs_{(S+As+Ce)} \quad (5)$$

In the second case, there is no inhibition of the reaction kinetic but there is a significant different between the signal obtained in mode A and B due to sample coloration or turbidity. Then, simplifying the Eq. (3) is possible in obtaining Eq. (6). In this case, it is also possible to calculate $[I^-]$ by Eq. (4) because the slope of an external calibration curve and the slope of a standard addition calibration in the sample are not significantly different.

$$Abs_{\text{iodide}} = Abs_{(S+W+Ce)} - Abs_{(S+As+Ce)} \quad (6)$$

In the third case, there is a matrix effect and also an inhibition of the reaction kinetic, i.e. due to a significant change of the pH in the final reaction mixture. Then, standard addition calibration is mandatory in order to quantify the iodide present in the sample. This means that for the calculation of $[I^-]$ using Eq. (4), “slope” corresponds to the slope of the standard addition curve, and Eq. (6) is used to calculate Abs_{iodide} (mode B and C).

In order to avoid quantification errors due to kinetic inhibition due to sample matrix, whenever possible, the calibration curve was done with synthetic sample matrix (e.g. synthetic seawater). Then, the reagent blank of the calibration was measured in mode C using a blank solution standard instead of water from S1 as done in mode A for milliQ water standards.

2.7. Real samples

Pharmaceutical products as well as coastal seawater samples were used to evaluate the applicability of the presented method to routine analysis. Four samples of coastal surface seawater from Palma (Mallorca, Balearic Islands, Spain) were collected and filtered through a 0.45 μm nylon membrane filter to separate any particulate matter and measured without further treatment.

In addition, the method was applied to the determination of two pharmaceutical formulations prescribed at acute iodine deficit, being Yodocefal (Italfarmaco S.A., Spain) and Pharmaton[®] Vit&Care (Boehringer Ingelheim España SA, Sant Cugat del Vallès, Spain). Both samples were nutritional supplements. Yodocefal is a lactose and corn-starch-based preparation with high contents of folic acid, B12 vitamin, and potassium iodide. Pharmaton[®] was a formulation of several vitamins and minerals including ascorbic acid and α -tocopherol as components with reductive potential in a matrix of hydroxypropylmethylcellulose, talc, iron oxide, triethyl citrate, and titanium dioxide among others.

One tablet of Yodocefal is equivalent to 200 μg of iodide (2000 $\mu\text{g g}^{-1}$), and Pharmaton[®] has 150 μg of iodine per tablet

(150 $\mu\text{g g}^{-1}$). From each product, 10 tablets were powdered and homogenized in a mortar. After that, 0.05 g of Yodocefal and 0.845 g of Pharmaton[®] were accurately weighed, transferred into 250 mL volumetric flasks and ultrasonically dissolved with 75 v/v % methanol: water for 1 h and after cooling down to room temperature made-up to volume. The obtained solutions were filtered through a 2.5 μm Whatman[®] 42 paper filter (Whatman[®] GmbH, Dassel, Germany) before use.

3. Results and discussion

3.1. Chip design and system configuration

A solution of 50 $\mu\text{g L}^{-1}$ of indigo carmine was used to determine the volumes required for filling the CHIP completely (225 μL) and to determine further dead volumes of connection tubing to the detection flow cell. The flow channels were of approximately 0.8 \times 0.8 mm id. Smaller flow channels would have been difficult to seal with the applied gluing technique without eventual blockage and would have required smaller syringe sizes or, using the chosen ones, have caused higher volumetric error.

To maximize the methods sensitivity, a five-fold larger syringe volume was used for sample handling, leading to a 5:1:1 volumetric ratio between sample, cerium reagent, and arsenite reagent. In order to minimize the consumption of reagents, both of them were injected into a slightly longer sample segment, thus applying the zone mixing flow concept instead of continuous confluent mixing. Baseline measurement was done with the detection flow cell filled with milliQ water. Injection of sample and reagents gave positive peak. Given the reaction coil volume, a sample volume of 160 μL was required for complete filling (225 μL 5/7) but a slightly larger volume of 190 μL was chosen to guarantee complete penetration of the reagent zone with sample.

Due to the slow reaction kinetic even in the presence of normal seawater iodide concentration, heating of the reaction mixture was required. Under the consideration of air bubble formation during this step, the detection cell was not integrated in the CHIP but an external cell was used to favor the redissolution of micro-bubbles in the reagent mixture at cooling.

3.2. Air bubble removal

Air bubbles present as one of the major problem in the unsegmented flow technique since they alter the flow and mixing pattern of the solutions, lead to baseline disturbances and false signals in several detection techniques, and affect further the precision of solution handling. The later effect is due to the compressibility of air bubbles leading to an effect of delay at the aspiration or dispense of solutions.

In flow techniques based on the use of syringe pumps such as in this work, air bubbles are generally caused by partly degassing of the solutions at the pressure drop during the aspiration of solutions for syringe refilling. In the present work, bubble formation was further possible due to degassing at the heating of the solution in the flow conduit. Small air bubbles trend to stack preferably on hydrophobic surfaces such as PTFE and can grow over time when air-saturated water is aspirated and becomes momentary super-saturated due to the pressure drop along the tube. Due to reduced bubble-stacking on hydrophilic surfaces, glass coils are used instead of polymer tubing in air-segmented flow techniques.

Elimination of stacked air bubbles can be achieved by increasing the flow velocity either by higher flow rate or by use of tubes of smaller diameter causing higher flow rates and shearing forces.

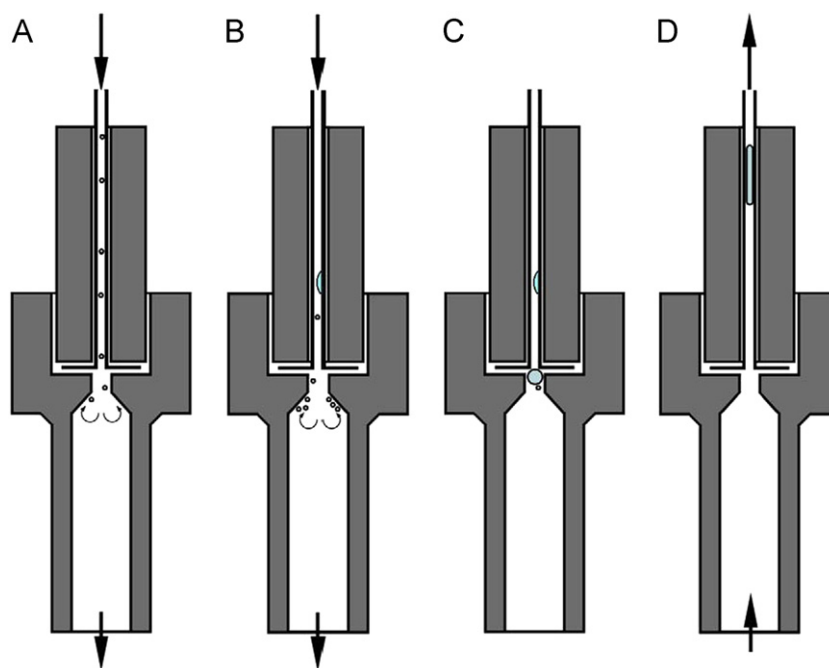


Fig. 3. Device for the trapping of air bubbles arising from negative pressure during refilling of the syringe. The device is placed between supply tube and syringe head valve position OFF (see Fig. 1). A and B: aspiration for syringe for refilling with accumulation of air bubbles behind the nozzle at the enlargement of the inner diameter. C: aggregation to larger bubbles at flow stop or operations in head valve position ON. D: discharge of the accumulated air by solution recycling.

Here, an improvement is the injection of an organic solvent in the carrier as demonstrated elsewhere [35]. Since the solvent shows a higher affinity to PTFE than water, wetting of the tube surface is improved and a lower flow rate is sufficient to overcome the reduced force the air bubble stacking. Another possibility is the injection of an air bubble of sufficiently large volume to act as segmentation and which can sweep stacked air bubbles at passing the tube.

High flow rates and the use of solvents were both impractical when using the PMMA flow conduit. On the other hand, degassing of solutions (by either helium passing, ultrasonification, or vacuum application) is effective if it is performed constantly and thus is generally costly. Therefore, air bubble trapping was used to eliminate the problems caused by bubble formation. The device developed for this task and its use are shown schematically in Fig. 3. The device consisted mainly of a rigid PVC tube, which was placed vertically on each head-valve position OFF (V1–V4). The tube leading to the respective solution reservoir was then connected on its top. At syringe refilling, the flow rate of the liquid inside the device is considerably reduced due to a significantly larger inner diameter than the connected supply tube. This allows the flotation of any formed air bubbles by the pressure drop during the aspiration step inside the device's void. Consequently, the air bubbles do not enter the syringe but aggregate to a single large bubble, which can be then expelled effectively to the solution reservoir after a certain number of measurements.

To further minimize the air bubbles stacking and thus accumulation in the syringes, the hydrophobic PTFE heads of the syringe pistons were coated with the hydrophilic PTFE derivate Nafion®. For this, a film of 5 wt% of Nafion® solution was applied onto each piston head and let dry over 30 min. This procedure was repeated twice. It was observed that air bubble stacking on the so-modified piston head was considerably reduced.

Both systems modifications led to a significant reduction of baseline disturbances and peak heights and peak shape reproducibility were improved greatly with RSD values of > 50% before and < 1.5% after application. The considerably large effect of both

counter-measurements can be explained due to several different affected mechanisms by air bubbles: (1) air bubbles changed the filling volume of the chip, so that in the worst case, part of the reaction mixture is not positioned reproducibly in the CHIP, (2) peak signals were disrupted by air bubbles, and (3) the mixture of all solutions is modified.

3.3. Optimization

3.3.1. Preliminary considerations

One of the principal objectives of this work was the determination of iodide at concentration levels as found in seawater. The total iodine level reported in seawater is in the range of $40 \mu\text{g L}^{-1}$ – $60 \mu\text{g L}^{-1}$ [19,23,36]. According to Lopez et al., approximately 80% of the total iodine in the seawater is presented as iodate and the other 20% as iodide. [23]. It is reported that the Sandell–Kolthoff reaction can be catalyzed by different iodine species such as iodine monochloride [37], iodide [16], and iodate, which can be reduced to iodide in the presence of arsenite in acidic medium [18,29]. However, some experiments we have performed with iodate demonstrate the iodate does not show a significant catalytic effect on Sandell–Kolthoff reaction (See Supplemental Material 1) as similarly reported elsewhere [18]. Taking into account this considerations, we decided to aim for a concentration working range of 10 – $100 \mu\text{g L}^{-1}$ (0.08 – $0.8 \mu\text{mol L}^{-1}$) of iodide. Therefore, the signal ratio between a blank and a standard solution of $50 \mu\text{g L}^{-1}$ of iodide was selected as desirability function of all optimization work. For the same reason, both solutions were prepared with synthetic seawater.

The absolute absorbance was impractical since it depended on the Ce(IV) concentration as well as to minor extend on acidity and incubation temperature. While the sensitivity was tunable by the choice of the analytical wavelength or longer reaction time, especially high precision of measurement was required to allow the differentiation of the very small variations for potential oceanographic application, here distinct seawater samples.

3.3.2. Acid

The influence of the final sulfuric acid concentration in the reaction mixture was studied from 2.9 mmol L^{-1} to 14.3 mmol L^{-1} corresponding to an acid concentration in both reagents of 0.01, 0.15, 0.27, 0.4, and 0.5 mol L^{-1} . It was observed that the higher acid concentration increased the peak height of both, the blank and the $50 \mu\text{g L}^{-1}$ iodide standard by the factor of 3 over the studied range (0.33 AU–0.99 AU).

This was most-likely due to the complex formation between Ce (IV) and acid. However, the signal ratio was hardly affected in the range from 7.7 to 14.3 mmol L^{-1} of final acid concentration with slightly prevalent maximum at 7.7 mmol L^{-1} . At the lowest acid concentrations tested, the reaction was practically insignificant.

Testing nitric acid as a promising alternative [19] to sulfuric acid, similar behavior of the reaction kinetic was observed considering the acid's equivalents without significant improvements. However, the absolute signal increase with increasing acid was low and remained at the level of blank (0.38 AU). A lower concentration of sulfuric acid leads similar yield than nitric acid and higher absolute signals. Then, sulfuric acid concentration was

optimized and a maximum signal was obtained at 0.27 mol L^{-1} . This concentration was set for the following experiments.

3.3.3. Temperature and reaction time

At the low iodide concentrations of interest, the catalyzed reaction between Ce(IV) and As(III) progresses nevertheless slowly. Thus a compromise between an acceptable sensitivity, i.e. long reaction times, and high sample throughput, i.e. short reaction times, had to be determined.

The influence of the reaction time on peak height was studied for 40–640 s at a temperature of 40.0°C . Experimental results are depicted in Fig. 4(A). It was observed that the blank signal decreased in approximation linearly and about 15% over a reaction time of 10 min. While for the standard, the decrease was of 87.5% over this range but decelerating as the reaction proceeded. Since it was estimated that linearity of the signal behavior would be lost with longer reaction times, a reaction time of 120 s was finally selected as an acceptable compromise, corresponding to a decrease of the standard signal of about 40%.

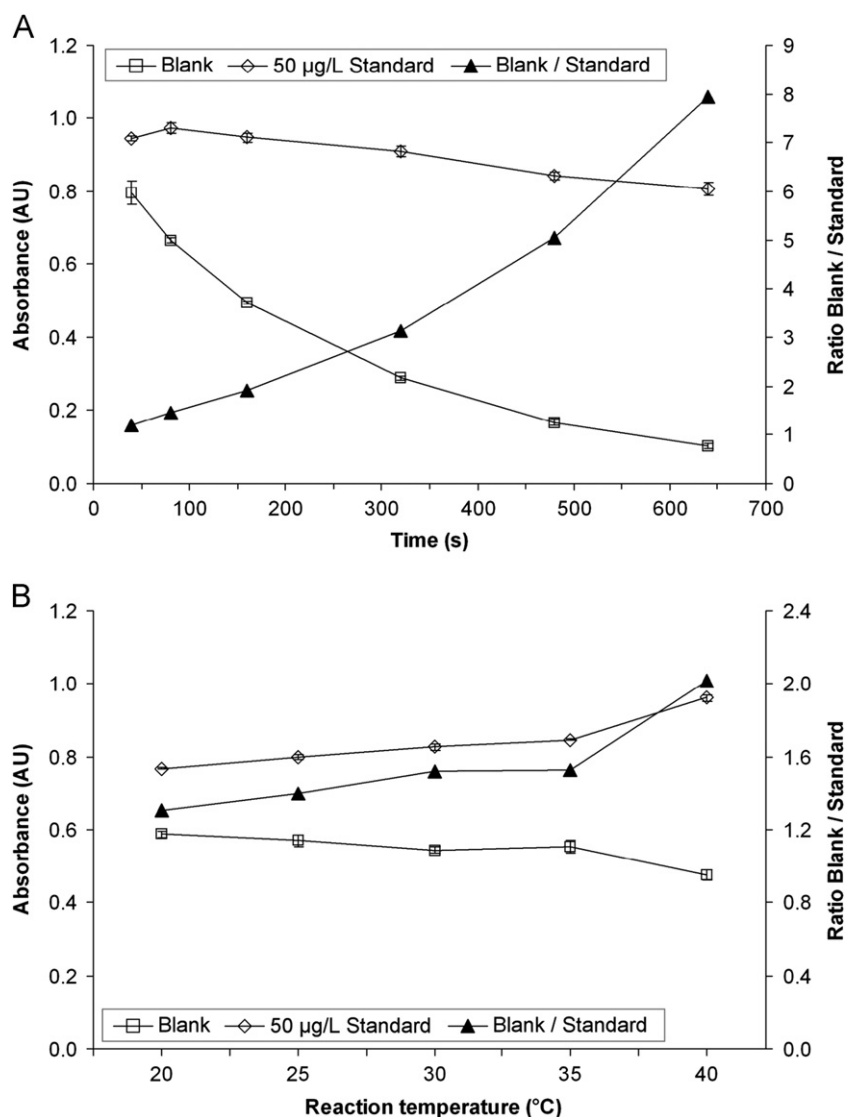


Fig. 4. Influence of the reaction time (A) and the incubation temperature (B) on the signal of blank and a $50 \mu\text{g L}^{-1}$ iodide standard as well as the ratio between of them (BL/ $50 \mu\text{g L}^{-1}$). Working conditions: 10 mmol L^{-1} of As(III), 3.5 mmol L^{-1} of Ce(IV), 270 mmol L^{-1} of H_2SO_4 , $150 \mu\text{L}$ of sample, flow rate 0.75 mL min^{-1} . Incubation temperature in A: 40°C in A. Reaction time in B: 160 s.

As it was expected, a higher reaction temperature increased the reaction rate greatly. The results are displayed in Fig. 4(B). In the studied range (20–40 °C), the blank/standard ratio increases from 1.3 at 20 °C to 2.0 at 40 °C. It was observed as a repeatable result, that the blank values increased with reaction temperature, which is most likely to the fact, that Ce(IV) forms dimers in acidic medium and by this changes its optical properties as former indicated elsewhere [38].

A higher sensitivity could be achieved with temperatures beyond the experimental domain i.e. at > 40 °C. However, higher temperature also increases the formation of air bubbles and thus can affect the methods reproducibility as reported elsewhere [39]. Therefore, the following work was continued using 40 °C as optimal reaction temperature.

3.3.4. Wavelength choice and reagent concentrations

The Ce(IV) concentration in reagent 1 is a key factor because it is the colored species and it defines the maximal signal i.e. the blank signal. In order to ensure compliance of the Lambert–Beer law, the maximal absorbance was kept lower than 1 AU. However, this value can also be adjusted by the selection of the analytical wavelength, i.e. a lower absorbance can be achieved by red-shifting the analytical wavelength and vice versa. On the other hand, the Ce(IV) concentration must be so high, that even after a 10-fold reduction of the signal by the catalytic activity of iodide, i.e. a final absorbance of about 0.1 AU, the rest concentration of cerium surpasses the concentration level of the highest aimed iodide standard (< 1 $\mu\text{mol L}^{-1}$) by far (i.e. factor < 100) to avoid the loss of linearity.

Finally, the noise level must be acceptable at the chosen wavelength, i.e. for the required measuring frequency, the blank value of aimed 1 AU still yields ideally between the range of 5–10% of the saturation level of the spectrometer. At lower light intensity, the baseline noise would increase; at higher intensity, saturation of the spectrometer during measurement of the highest aimed standard is probable.

The emission intensity of the used light source decreased rapidly to beyond 380 nm. At shorter wavelengths, the organic matter dissolved in seawater samples would have caused a significant contribution to the blank value while longer wavelength would have caused loss of sensitivity. Therefore, 380 nm was chosen as analytical wavelength allowing measurement readings at 5 Hz with a baseline noise in the range of 1E^{-3} AU (about 90% of saturation). The applicable Ce(IV) concentration was found to be in the order of 3.5 mmol L^{-1} giving a blank value of 0.94 AU. The sensitivity, i.e. the blank to standard signal ratio, did not alter significantly over the studied range of 3–4.25 mmol L^{-1} and thus, 3.5 mmol L^{-1} Ce(IV) concentration was selected for all the following work.

Reaction Eqs. 1 and 2 indicate a stoichiometric factor between As(III) and Ce(IV) of 1–2. Former works recommend the use of an excess of As(III) to this ratio [18,24,29]. Therefore, the

concentration of As(III) was studied in the range 10–40 mmol L^{-1} . No significant effect on the signal ratio of blank and standard was observed, so the lowest concentration of 10 mmol L^{-1} was set for the following experiments.

3.4. Figure of merits

Using the optimal conditions, i.e. 10 mmol L^{-1} of As(III), 3.5 mmol L^{-1} of Ce(IV), 270 mmol L^{-1} of H_2SO_4 and a reaction time of 120 s at 40 °C, a linear calibration range was found of up to $75\text{ }\mu\text{g L}^{-1}$ of iodide corresponding to approximately 40% of initial Ce(IV) concentration left. For higher concentrations, the reaction kinetic speed was found to be decreasing.

The average repeatability of all standard and sample measurements was $1.5 \pm 1\%$. This relative low value was achievable after the reduction of the air bubbles with the measurements described in Section 3.2.

The calibration curve function using synthetic seawater standards was Peak height = $-6.56 \pm 0.26\text{ mAU L }\mu\text{g}^{-1}$ [Iodide] + $0.904 \pm 0.075\text{ AU}$ ($n=6$). For MilliQ water standards, significant lower intercept and slope were found with Peak height = $-5.19\text{ mAU L }\mu\text{g}^{-1}$ [Iodide] + 0.609 AU .

Values for limit of detection (LOD) were calculated from the threefold standard deviation of 10 consecutive blank measurements divided by the calibration curve slope. For synthetic seawater standards measured at three different days, a LOD of $4.7 \pm 2.1\text{ }\mu\text{g L}^{-1}$ was found. From milliQ calibration curve and blank measurements, a LOD level of $4.4\text{ }\mu\text{g L}^{-1}$ was calculated.

The entire analytical procedure lasted about 152 s, enabling a frequency of injection of 23 h^{-1} . Solution consumption was low with 190 μL of sample, 38 μL of Ce(IV) and 38 μL of As(III) solution corresponding to 0.38 μmol of As(III) and 0.13 μmol of Ce(IV) leading to a very low reagent cost per analysis.

A comparison with former methods using the same methodology is summarized in Table 2. The first three works used the Sandell–Kolthoff reaction [24,29,40], two of them use flow-based systems to carry out the analysis. The proposed system was achieved similar or better LOD, repeatability, and sample throughput than those compared. An important improvement was especially achieved in respect of reagent and sample consumption, which was related to the use of the CHIP device. For example, the quantity of arsenic used per injection was reduce 3, 10 and 100 time respectively in the present work, and a similar result was obtained for cerium reagent. Other spectrophotometric methods for iodide determination which use a different reagent than Sandell–Kolthoff reaction, is also compared. [25,28]. These methods present a high injection throughput due to the use of FIA, but to the cost of sensitivity. These methods just can quantify milligram per liters of iodide. This fact demonstrates that the Sandell–Kolthoff reaction has been one of the most sensitive and selective reaction for the determination of trace levels of iodide.

Table 2

Figure of merit and experimental characteristics of spectrophotometric iodide determination. Comparison with similar methods reported.

Ref.	Reaction	λ_{max} (nm)	System	LOD ($\mu\text{g L}^{-1}$)	Working range ($\mu\text{g L}^{-1}$)	RSD, % ($\mu\text{g L}^{-1}$)	T (°C)	Injection (h $^{-1}$)	As(III) (μmol)	Ce(IV) (μmol)
[40]	As(III) + Ce(IV)	410	SIA	3	10–200	3.6%	45	15	3	0.96
[29]	As(III) + Ce(IV)	420	FI	9.3	100–800	0.72% (800)	–	26	10	1.25
[24]	As(III) + Ce(IV) + DPASA	750	Batch	2	5.0–60	12% (50)	30	< 10	100	5
[25]	Pyrocate. Violet	550	FIA	300	(5–25) · 10^{-3}	4% (1000)	45	46	–	–
[28]	Cr ₂ O ₇ ²⁻	355	FIA	200	(5–400) · 10^{-3}	2% (5000)	–	50	–	–
Present work	As(III) + Ce(IV)	380	MSFIA	4.7	4.7–75	1.2% (30)	40	23	0.38	0.133

3.5. Sample analysis and interferences

The applicability of the proposed method was evaluated by the determination of iodide in five coastal seawater samples and aqueous extracts of two medicaments.

The calibration standards for the analysis of seawater samples were prepared with synthetic seawater [30] to compensate the interferences of other halides (F^- , Cl^- , and Br^-) as well as the optical effect due to the higher refraction index of seawater as studied elsewhere [36]. The calibration curve was done in the range of 30–70 $\mu g L^{-1}$, i.e. the typical range of total concentration of iodine in seawater [36]. Each seawater sample was spiked with 15 and 30 $\mu g L^{-1}$ of iodide to evaluate the accuracy of the method. The mean slope obtained for the samples was -6.38 ± 0.14 mAU $L \mu g^{-1}$ and by this no significant difference from the slope was obtained with synthetic seawater calibration standards of -6.56 ± 0.26 mAU $L \mu g^{-1}$ (compare representation in Fig. 5A). In conclusion, there is no significant difference in the reaction kinetic between the seawater samples and synthetic seawater.

The recovery values calculated from the two spike levels and synthetic seawater calibration standards were between 96% and 106% with the data given in Table 3. It should be pointed out that the sample blank values obtained in measurement mode B were insignificant compared to the blank standard obtained in mode C for synthetic seawater (blank of calibration standards).

The results indicate that the effect of the seawater matrix can be neglected if synthetic seawater is used for the calibration. Under this condition, the method is applicable for the determination of iodide in real seawater samples. On the other hand, the use of milliQ standards is imperative for samples of low salt content.

Also, two pharmaceutical samples were used to evaluate the applicability of the proposal method to matrices with high content of reducing compounds. Standard addition calibration was required due to the unknown effect of the sample matrix in comparison with a calibration prepared with milliQ standards. The results are depicted in Fig. 5(B). Sample blank values (mode B) were 2.6% and 20.2% lower than the reagent blank (mode A) indicating a significant unspecific reduction of Ce(IV) by the

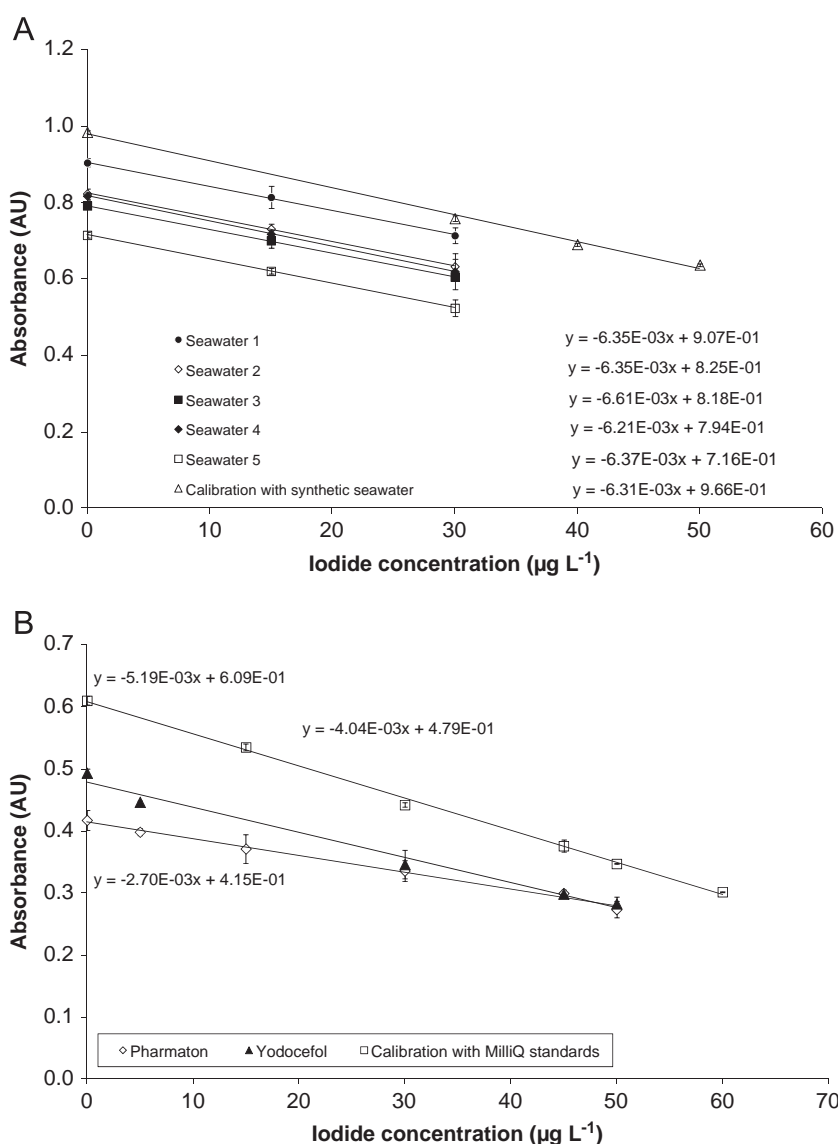


Fig. 5. Samples evaluation. (A) Calibration for seawater samples and synthetic seawater. (B) Standard addition on pharmaceutical preparations. Working conditions: 10 mmol L^{-1} of As(III), 3.5 mmol L^{-1} of Ce(IV), and 270 mmol L^{-1} of H_2SO_4 , 40 °C reaction temperature, 150 μL of sample, flow rate of 0.75 $mL min^{-1}$, and reaction time of 120 s.

Table 3

Iodide contents in seawater working conditions: 10 mmol L⁻¹ of As(III), 3.5 mmol L⁻¹ of Ce(IV), and 270 mmol L⁻¹ of H₂SO₄, at 40 °C, using 38 µL of samples at 0.75 mL min⁻¹, and 120 s of reaction time.

Seawater calibration and sample	Absorbance (AU)	Iodide added (µg L ⁻¹)	Iodide found (µg L ⁻¹)	Recovery (%)	Slope (AU L µg ⁻¹)
SSW calibration	0.986	0			
	0.760	30			-0.00631
	0.692	40			
	0.638	50			
SW1	0.905	0	9.61		
	0.815	15	23.95	96	-0.00635
	0.715	30	39.88	101	
	0.824	0	22.46		
SW2	0.732	15	37.11	98	-0.00635
	0.634	30	52.70	101	
SW3	0.819	0	23.40		
	0.719	15	39.25	106	-0.00661
	0.620	30	54.85	105	
	0.793	0	27.47		
SW4	0.702	15	41.98	97	-0.00621
	0.607	30	57.06	99	
SW5	0.716	0	39.70		
	0.622	15	54.68	100	-0.00637
	0.525	30	70.04	101	

matrix of Pharmaton[®]. This proves the usefulness of the current approach allowing additional measurement of each sample's blank by changing the measurement mode.

As expected, the slope values obtained from standard addition were significantly lower for both Yodocefal (-22.2%) and Pharmaton[®] (-48.0%). The iodide concentration measured was inside the permissible range reported by the pharmaceutical formulation for both medicaments with 2050 ± 22 µg g⁻¹ found and 2000 ± 100 µg g⁻¹ reported for Yodocefal; and 155 ± 4 µg g⁻¹ found and 150 ± 7.5 µg g⁻¹ reported for Pharmaton[®]. Recovery values from standard addition were 99% and 104% indicating a well applicability of the proposed method and analyzer for these kinds of formulations.

Generally, the Sandell–Kolthoff reaction is known as selective and sensitive for the determination of iodide in different matrix samples. Nonetheless, various interferences have already been described by Sandell and Kolthoff themselves and later researchers [16,41].

Ru(IV) and Os(VIII) cations show a similar behavior as iodide [16] but present hardly any obstacle in natural water samples due to their low concentration level. Low interference but with significant impact for seawater samples are other halides such as chloride, because it can be oxidized by Ce(IV). However this reaction between Ce(IV) and Cl⁻ is significantly slower than the main reaction (Ce(IV) and As(III)). [42]. Nevertheless, synthetic seawater was used in this work for calibration in order to correct the matrix effect including the Cl⁻ concentration.

While metal cations, which form insoluble complexes with iodide such as Ag(I) and Hg(II) can hardly be eliminated and present relevant interferences, redactors reducing agents such as thiocyanate, ascorbic acid, or glucose can be eliminated by sample pretreatment or, as done in this work, evaluated by sample blank measurement [31,40]. Others iodine ions, as iodate, are reduced by As(III) in acid media [18], so that the use of an excess of As(III) guarantee the determination of total free iodine expressed as iodide.

4. Conclusions

The proposed system proved to allow accurate, sensitive, selective and reliable determination of iodide in both seawater

samples as well as in nutrient supplement formulations by automation of the Sandell–Kolthoff reaction. The analyzer system shows the required characteristics such as simplicity, compactness, and portability, for oceanographic on-board application for the analysis of iodide in seawater. By this, any problems related to sample transportation can be avoided. By the use of a heated monolithic flow conduit coupled to a versatile multisyringe pump, similar or better analytical performance than former reported were achieved using a significantly reduced amounts of reagents. Subsequent measurement of the analyte specific and unspecific signal was feasible by using four syringes for sample, reagents, and water handling. Two approaches for the elimination of air bubble problems were firstly described and have allowed highly reproducible measurements.

Acknowledgments

This work was funded by the Government of the Balearic Islands by Project 43/2011 (FEDER funds) and the Spanish Ministry of Science and Innovation (MICINN) by Project CTQ2010-15541. F. Zohra was funded by the Averroes Grants of the Europe Union. C. Henríquez is very grateful with the “Conselleria d'Educació, Cultura i Universitat” and the “European Social Fund” for funding her PhD Grant. B. Horstkotte was funded by the Postdoctoral Program OPVK 2.3 (CZ.1.07/2.3.00/30.002) of the Ministry of Education, Youth and Sport of the Czech Republic.

Appendix A. Supporting information

Supplementary data associated with this article can be found in the online version at <http://dx.doi.org/10.1016/j.talanta.2013.02.072>.

References

- [1] B. Horstkotte, O. Elsholz, V. Cerdà, J. Flow Injection Anal. 22 (2005) 99–109.
- [2] V. Cerdà, J.M. Estela, R. Forteza, A. Cladera, E. Becerra, P. Altimira, P. Sitjar, Talanta 50 (1999) 695–705.
- [3] V. Cerdà, J. Avivar, C.A., Pure Appl. Chem. 84 (2012) 1983–1998.
- [4] A. Cerdà, V. Cerdà, An introduction to flow analysis, SCIWARE, S.L. ed., Crison Instruments, S.A., Barcelona, Spain, 2009.
- [5] M. Trojanowicz, Flow Injection Analysis. Instrumentation and applications, World Scientific Publishing Co. Pte. Ltd, Farrer Road, Singapore, 2000.
- [6] S.D. Kolev, I.D. McKelvie, Adv. Flow Injection Anal. Relat. Tech. (2008).
- [7] E.H. Hansen, FIALab, Bellevue, 2012.
- [8] J. Ruzicka, G.D. Marshall, Anal. Chim. Acta 237 (1990) 329–343.
- [9] C.E. Lenehan, N.W. Barnett, S.W. Lewis, Analyst 127 (2002) 997–1020.
- [10] F. Altburt, B. Horstkotte, A. Cladera, V. Cerdà, Analyst 124 (1999) 1373–1381.
- [11] J. Růžicka, E.H. Hansen, Anal. Chim. Acta 161 (1984) 1–25.
- [12] E.R. Rodrigues, R.A. Lapa, Anal. Sci. 25 (2009) 443–448.
- [13] C.S. Martinez-Cisneros, N. Ibanez-Garcia, F. Valdes, J.C. Alonso, Anal. Chem. 79 (2007) 8376–8380.
- [14] B. Horstkotte, C.M. Duarte, C.V., Anal. Chim. Acta, Submitted for publication.
- [15] J. Ruzicka, Analyst 125 (2000) 1053–1060.
- [16] E.B. Sandell, I.M. Kolthoff, J. Am. Chem. Soc. 56 (1934) 1426–1428.
- [17] J. Stanley, H.C. Thomas, Sterling Chem. Lab. 78 (1956) 3950.
- [18] C.P. Shelor, P.K. Dasgupta, Anal. Chim. Acta 702 (2011) 16–36.
- [19] J.S. Edmonds, M. Morita, Pure Appl. Chem. 70 (1998) 1567–1584.
- [20] V.V. Kuznetsov, V.Y. Ermolenko, L. Seffar, J. Anal. Chem. 59 (2004) 688–693.
- [21] V.V. Kuznetsov, V.Y. Ermolenko, L. Seffar, J. Anal. Chem. 62 (2007) 479–485.
- [22] H.-F. Li, C.-G. Xie, J. Lumin. 132 (2012) 30–34.
- [23] J. Lopez, Fundamentos de Química Oceanográfica, Cádiz, 1989.
- [24] O.M. Trokhimenko, N.V. Zaitsev, J. Anal. Chem. 59 (2004) 491–494.
- [25] A. Cerdà, R. Forteza, V. Cerdà, Food Chem. 46 (1993) 95–99.
- [26] F. Grases, R. Forteza, J.G. March, V. Cerdà, Talanta 32 (1985) 123–126.
- [27] V.T.P. Nguyen, V. Piersoel, T. El Mahi, Talanta 99 (2012) 532–537.
- [28] J.T. Hakedal, P.K. Egeberg, Analyst 122 (1997) 1235–1237.
- [29] N. Choengchan, K. Lukkanakul, N. Ratanawimarnwong, W. Waiyawat, P. Wilairat, D. Nacapricha, Anal. Chim. Acta 499 (2003) 115–122.
- [30] M.A.H. Franson, L.S. Clesceri, A.E. Greenberg, R. Rhodes Trussell, in: D.d.S.S.A. (Ed.), APAH, AWWA and WPCF, 1992.

- [31] T. Masadome, R. Sonoda, Y. Asano, *Talanta* 52 (2000) 1123–1130.
- [32] Z. Huang, Z. Zhu, Q. Subhani, W. Yan, W. Guo, Y. Zhu, *J. Chromatogr. A* 1251 (2012) 154–159.
- [33] G.A. Ubom, Y. Tsuchiya, *Water Res.* 22 (1988) 1455–1458.
- [34] K. Ito, T. Ichihara, H. Zhuo, K. Kumamoto, A.R. Timerbaev, T. Hirokawa, *Anal. Chim. Acta* 497 (2003) 67–74.
- [35] B. Horstkotte, C. Arnau, F. Valero, O. Elsholz, V. Cerda, *Biochem. Eng. J.* 42 (2008) 77–83.
- [36] V.W. Truesdale, P. Chapman, *Mar. Chem.* 4 (1976) 29–42.
- [37] I.M. Kolthoff, E.B. Sandell, E.J. Meehan, S. Bruckenstein, *Análisis Químico Cuantitativo*, Librería y Editorial Nigar Madrid, 1972.
- [38] F. Bermejo Martínez, *Tratado de Química Analítica general cuantitativa e instrumental*, 5ta ed., Santiago de Compostela, 1974.
- [39] B. Horstkotte, E. Werner, S. Wiedemeier, O. Elsholz, V. Cerda, R. Luttmann, *Anal. Chim. Acta* 559 (2006) 248–256.
- [40] J.A. Erustes, R. Forteza, V. Cerda, *J. AOAC Int.* 84 (2001) 337–341.
- [41] P.A. Rodriquez, H.L. Pardue, *Anal. Chem.* 41 (1969) 1376–1380.
- [42] R.B. Fischer, D.G. Peters, *Análisis Químico Cuantitativo*, Editorial Interamericana, Mexico DF, 1970.